J Math Chem (2009) 46:1271–1291
DOI 10.1007/s10910-008-9516-y

ORIGINAL PAPER

Mechanics of nanoscale orbiting systems

Yue Chan · Ngamta Thamwattana · Grant M. Cox · James M. Hill

Received: 12 November 2008 / Accepted: 8 December 2008 / Published online: 6 January 2009

Abstract At the nanoscale a number of very high frequency oscillating systems involving relative motion with respect to a carbon nanotube have been identified. In this paper, we study the two-body systems of an atom and a fullerene C_{60} orbiting around a single infinitely long carbon nanotube and a fullerene C_{60} orbiting around a fullerene C_{1500}. The van der Waals interaction forces are modeled using the Lennard–Jones potential together with the continuum approach for which carbon atoms are assumed to be uniformly distributed over the surfaces of both the fullerenes and the carbon nanotube. Some analytical and perturbation solutions are obtained for the regime where the attractive term of the potential energy dominates. Certain circular orbiting radii of these nanoscale systems are estimated using a stability argument and the corresponding circular orbiting frequencies can then be calculated by investigating the minimum energy configuration of their effective potential energies. We find that the circular orbiting frequencies of the various proposed nano-systems are in the gigahertz range. Finally, the classification of their orbiting paths is determined numerically.

Keywords Fullerenes · Carbon nanotubes · Orbiting systems · Lennard–Jones · Gigahertz frequency

Y. Chan (✉) · N. Thamwattana · G. M. Cox · J. M. Hill
Nanomechanics Group, School of Mathematics and Applied Statistics,
University of Wollongong, Wollongong, NSW 2522, Australia
e-mail: yc321@uow.edu.au

N. Thamwattana
e-mail: ngamta@uow.edu.au

1 Introduction

The discovery of carbon nanotubes [1] has led to many theoretical, computational and experimental studies on their properties and various ways to create new possible carbon nanotube based devices. One such device is the nanoscale oscillator, for which the oscillation of a carbon molecule (a fullerene C_{60} or a carbon nanotube) inside a carbon nanotube can generate frequencies in the gigahertz range. The concept of nanoscale oscillators is based upon the experiments of Cumings and Zettl [2] on multi-walled carbon nanotubes, where they remove the cap from one end of the outer shell and attach a moveable nanomanipulator to the core in a high-resolution transmission electron microscope. By pulling the core out and pushing it back into the outer shell, they report an ultra-low sliding frictional force, which is also confirmed by Yu et al. [3]. Further, Cumings and Zettl [2] observe that the extruded core, after release, quickly and fully retracts inside the outer shell due to the restoring force resulting from the van der Waals interaction acting on the extruded core. These experimental results led to the molecular dynamics studies of Zheng and Jiang [4] who show that the oscillating of the inner shell between the open ends of the outer shell of a multi-walled carbon nanotube generates a frequency in the gigahertz range. Molecular dynamics simulations undertaken by Legoas et al. [5], Rivera et al. [6,7] and others also confirm such gigahertz frequency phenomena. In terms of a mathematical modelling perspective, Baowan and Hill [8] investigate the force distribution for a double-walled carbon nanotube oscillator by utilizing the continuum approach for the Lennard–Jones potential together with Newton's second law assuming a frictionless environment. They obtain an analytical expression for the interaction force and their model also predicts the gigahertz oscillatory behavior for the double-walled carbon nanotube oscillators.

Further, Zheng and Jiang [4] suggest that the oscillatory frequency increases as the inner oscillating tube becomes shorter. This result leads to the molecular dynamics study of Liu et al. [9] on the oscillation of a C_{60} fullerene inside a single-walled carbon nanotube. While Liu et al. [9] focus on the oscillation frequency, the study of Qian et al. [10] concerns the suction and the repulsion of a C_{60} molecule at the vicinity of the tube's open end and the velocity of the molecule after being sucked into the nanotube. Based on the molecular dynamics simulations of both Liu et al. [9] and Qian et al. [10], Cox et al. [11,12] develop a mathematical model employing fundamental mechanical principles and classical applied mathematical techniques to determine the acceptance condition and the suction energies of the C_{60} fullerene upon entering a nanotube. They determine the minimum radius of a carbon nanotube for which the C_{60} fullerene will be accepted from rest and the maximum total energy once the C_{60} molecule is sucked inside the nanotube by the van der Waals forces. In addition, Cox et al. [11,12] show that the gigahertz oscillating behavior arises from the two peak-like forces operating at the nanotube's open ends. The analytical model of Cox et al. [11,12] is also extended to examine a more complicated structure of the gigahertz oscillators, including the nanotube bundle oscillators for which the oscillating molecule inside the bundle is either a single nanotube or a C_{60} fullerene [13,14].

For other types of nanoscale oscillators, Hilder and Hill [15,16] find that the gigahertz frequencies can also be obtained from a sector of a nanotorus orbiting inside a carbon nanotorus and an atom and a C_{60} fullerene orbiting inside a nanotorus. In this

paper, we further investigate orbiting phenomenon at the nanoscale. In particular, we consider an atom and a C_{60} fullerene orbiting around the outside a carbon nanotube and also a C_{60} fullerene orbiting around a C_{1500} molecule. The van der Waals interaction energy is modelled using the 6–12 Lennard–Jones potential and the continuum approach for which we assume a uniform distribution of carbon atoms on the surfaces of the carbon nanotube and the fullerene. We find that the interacting molecules move relatively with respect to each other under the influence of their mutual central force. While their loci cannot be integrated in terms of well-known special functions, they can be determined by the numerical evaluation of certain integrals. Some analytical and perturbation solutions are sought, where the attractive forces dominate and assuming that the total energies of both the atom and the fullerene are small, and these special analytical results provide some insight into suitable forms of the loci. Finally, the circular radii are estimated by finding the minimum energy configuration of their effective potential energies, and a stability analysis is employed to ensure the stability of the circular radii, which is of practical importance in creating certain nano-devices. For all cases, the circular orbiting frequencies reach the gigahertz range. We comment that this paper ignores any thermal fluctuations arising from the environment. If such effects are incorporated, the orbiting motion of these systems may be critically disrupted and the orbiting phenomenon might not be observed.

The paper is structured as follows. In the following section, we give the basic equations of motion for a two-body problem. In Sects. 3 to 5, an atom–carbon nanotube system, a fullerene–carbon nanotube system and a fullerene–fullerene system are examined, respectively. For all cases, the classification of their loci, in terms of both numerical and analytical investigations is given, and their circular orbiting frequencies are provided.

2 Equations of motion

In this section, a brief description of the equations of motion for a two-body problem is presented. A more detailed derivation and explanation can be found in many classical mechanics graduate textbooks, such as [17]. For a system of two objects, the connecting potential energy $V(\boldsymbol{r})$ depends only on the relative displacement between the two objects $\boldsymbol{r} = \boldsymbol{r_2} - \boldsymbol{r_1}$, where $\boldsymbol{r_1}$ and $\boldsymbol{r_2}$ denote the position vectors of the two masses m_1 and m_2 relative to their center of mass respectively (it is essential for a central force problem that the potential energy between two bodies depends only on $\boldsymbol{r}$). Thus, let $\boldsymbol{P}$ denote the position vector of the center of mass and the Lagrangian for the two-body problem is defined by

$$L = T(\dot{\boldsymbol{P}}, \dot{\boldsymbol{r}}) - V(\boldsymbol{r}), \tag{1}$$

where T and V denote the kinetic and the potential energies respectively. The total kinetic energy T can be expressed as the sum of the kinetic energy owing to the motion of the center of mass and the kinetic energy owing to the motion about the center of mass. That is,

$$T = \frac{1}{2}M\dot{\boldsymbol{P}}^2 + \frac{1}{2}m_1\dot{\boldsymbol{r}}_1^2 + \frac{1}{2}m_2\dot{\boldsymbol{r}}_2^2, \tag{2}$$

where $M = m_1 + m_2$ is the total mass of the two-body system. The two position vectors can then be related to the relative displacement vector $\boldsymbol{r}$ by

$$\boldsymbol{r}_1 = -\frac{m_2}{m_1 + m_2}\boldsymbol{r}, \qquad \boldsymbol{r}_2 = \frac{m_1}{m_1 + m_2}\boldsymbol{r}, \tag{3}$$

which upon substituting Eqs. 3 and 2 into Eq. 1, the Lagrangian can be rewritten as

$$L = \frac{1}{2}M\dot{\boldsymbol{P}}^2 + \frac{1}{2}m\dot{\boldsymbol{r}}^2 - V(\boldsymbol{r}), \tag{4}$$

where $m = m_1m_2/(m_1 + m_2)$ is called the reduced mass of the system. Therefore, the two-body problems can always be reduced to the reduced mass m, moving about the center of mass of the system as is incorporated in Eq. 4. If we assume $V(\boldsymbol{r}) = V(r)$ and express the Lagrangian in terms of polar coordinates, then Eq. 4 becomes

$$L = \frac{1}{2}m(\dot{r}^2 + r^2\dot{\theta}^2) - V(r), \tag{5}$$

and the angular momentum of the system is obtained from L by $p = \partial L/\partial\dot{\theta} = mr^2\dot{\theta}$. Without any external torque, it is known that the angular momentum of the system is conserved, so that

$$h = mr^2\dot{\theta}, \tag{6}$$

where h denotes an arbitrary constant. Finally, the total energy E is given by

$$E = \frac{1}{2}m(\dot{r}^2 + r^2\dot{\theta}^2) + V(r) = \frac{1}{2}m\dot{r}^2 + \frac{h^2}{2mr^2} + V(r) = \frac{1}{2}m\dot{r}^2 + V_{eff}(r), \tag{7}$$

where $V_{eff}(r) = h^2/2mr^2 + V(r)$ denotes the effective potential energy, which comprises both the angular kinetic energy $h^2/2mr^2$ and the potential energy $V(r)$. A circular orbit of radius R can be computed by finding the minimum energy configuration of V_{eff}.

3 Atom–carbon nanotube system

In this section, we investigate a single carbon atom orbiting around a thin infinitely long carbon nanotube, approximated by a line, under the influence of the van der Waals force. Using the 6–12 Lennard–Jones potential and the continuum approach, the van der Waals interaction energy of this system is given by

$$V(\rho) = n_g\int_{-\infty}^{\infty}\left(\frac{-A}{\rho^6} + \frac{B}{\rho^{12}}\right)dz, \tag{8}$$

Table 1 Numerical values of constants used in the model

Radius of (6,6)	$a = 4.071\,\text{Å}$
Radius of C_{60}	$b = 3.55\,\text{Å}$
Radius of C_{1500}	$c = 17.5225\text{Å}$
Carbon–carbon bond length	$\sigma = 1.421\,\text{Å}$
Mean surface density of a single layer graphene	$n_g = 0.3812\,\text{Å}^{-2}$
Mean surface density of C_{60}	$n_1 = 0.3789\,\text{Å}^{-2}$
Mean surface density of C_{1500}	$n_2 = 0.3888\,\text{Å}^{-2}$
Mass of a single carbon atom	$m_a = 1.993 \times 10^{-26}$ kg
Mass of a single C_{60} fullerene	$m_1 = 1.196 \times 10^{-24}$ kg
Mass of a single C_{1500} fullerene	$m_2 = 2.9895 \times 10^{-23}$ kg
Attractive constant	$A = 17.4\,\text{eV}\,\text{Å}^6$
Repulsive constant	$B = 29 \times 10^3\ \text{eV}\,\text{Å}^{12}$

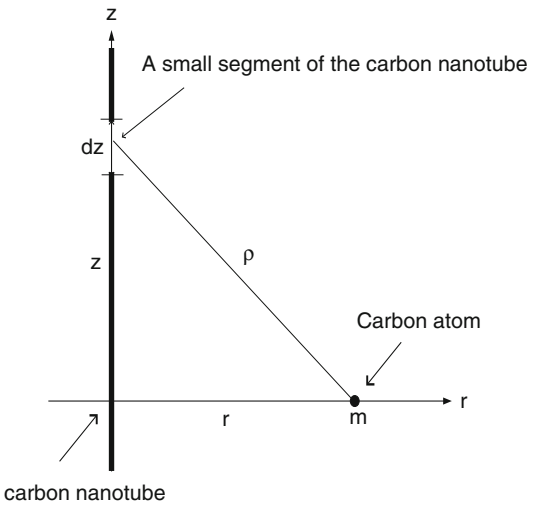

Fig. 1 Atom–carbon nanotube system

where A and B are the attractive and repulsive constants, respectively, ρ denotes the distance between the orbiting atom and an arbitrary atom on the carbon nanotube, and n_g is the mean surface density of atoms on the carbon nanotube. The numerical values of the constants used throughout this paper are presented in Table 1.

From Fig. 1, we have $\rho^2 = z^2 + r^2$ so that the molecular potential energy $V(r)$ can be expressed as

$$V(r) = n_g \int_{-\infty}^{\infty} \left\{ \frac{-A}{(z^2 + r^2)^3} + \frac{B}{(z^2 + r^2)^6} \right\} dz, \tag{9}$$

which upon making the substitution $z = r \tan\theta$, Eq. 9 becomes

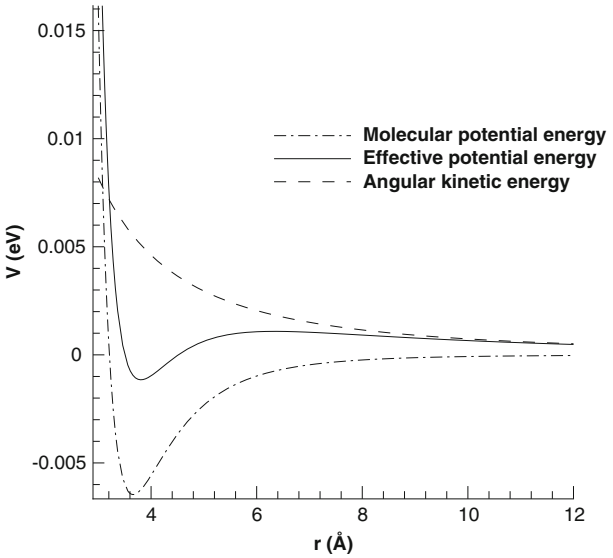

Fig. 2 Comparison between angular kinetic energy, molecular potential energy and effective potential energy for atom–carbon nanotube system

$$V(r) = n_g \int_{-\pi/2}^{\pi/2} \left\{ -\frac{A}{r^5} \cos^4\theta + \frac{B}{r^{11}} \cos^{10}\theta \right\} d\theta = -\frac{A'}{r^5} + \frac{B'}{r^{11}}, \tag{10}$$

where $A' = 3\pi n_g A/8 = 7.8\,\text{eV}\,\text{Å}^4$ and $B' = 63\pi n_g B/256 = 8547\,\text{eV}\,\text{Å}^{10}$ are the modified attractive and repulsive constants respectively. This potential energy is illustrated graphically in Fig. 2. According to Eq. 7, the effective potential energy $V_{eff}(r)$ is given by

$$V_{eff}(r) = \frac{C'}{r^2} - \frac{A'}{r^5} + \frac{B'}{r^{11}}, \tag{11}$$

where $C' = h^2/2m$. The extra term C'/r^2 corresponds to the atom's angular kinetic energy. The classification of the atom's loci can then be obtained by analyzing the total energy of the system, which from Eqs. 7 and 11 becomes

$$E = \frac{1}{2} m\dot{r}^2 + \left(\frac{C'}{r^2} - \frac{A'}{r^5} + \frac{B'}{r^{11}} \right), \tag{12}$$

and upon changing the coordinate system from t to θ by utilizing Eq. 6, we obtain

$$d\theta = \frac{\sqrt{C'}\,dr}{r^2\sqrt{E + A'/r^5 - B'/r^{11} - C'/r^2}}. \tag{13}$$

We can simplify the above equation by making the substitution $u = r^{-1}$, and by integrating both sides of Eq. 13 to yield

$$\theta - \theta_0 = -\int \frac{\sqrt{C'}du}{\sqrt{E - B'u^{11} + A'u^5 - C'u^2}}. \tag{14}$$

Unlike the classical two-body problem, for which the polynomial under the square root is a quadratic, in this case the polynomial under the square root has a maximum degree of 11, which makes the integration much harder to effect in terms of well-known special functions. Thus, some numerical and perturbation methods are presented in order to gain some physical insight into this problem. The atom's orbiting circular radius can be readily computed by finding the minimum energy configuration of the effective potential energy. Since, there is a one-to-one relationship between its circular orbiting radius and its circular orbiting frequency (15), in the following subsection the circular orbiting frequency of this system is estimated and it is found to be operating in the gigahertz range.

3.1 Circular orbiting frequency of atom–carbon nanotube system

In this section, the circular orbiting frequency of an atom orbiting around a carbon nanotube is estimated by examining the minimum energy configuration of the effective potential energy, since it can be shown from classical mechanics that the minimum energy configuration of Eq. 11 corresponds to a circular orbit of the atom. By solving $V'_{eff}(r) = 0$, the circular angular frequency, ω, is given by

$$\omega^2 = \frac{5A'}{mR^7} - \frac{11B'}{mR^{13}}, \tag{15}$$

where R is the atom's circular orbiting radius. In order to obtain Eq. 15, the conservation of angular momentum of the system is utilized. Note that Eq. 15 by itself is not sufficient to determinate the circular orbiting frequency of the atom. However, the stability of a nearly circular orbit and the boundness of the atom's locus at R have to be satisfied for the atom to keep orbiting in its circular orbit. To determine the stability of the atom's circular orbit, differentiating both sides of Eq. 12 with respect to t, yields

$$m\ddot{r} + \left(-\frac{2C'}{r^3} + \frac{5A'}{r^6} - \frac{11B'}{r^{12}}\right) = 0, \tag{16}$$

so that upon making the substitution $u = 1/r$, we get

$$\frac{d^2u}{d\theta^2} - \frac{m}{h^2}(5A'u^4 - 11B'u^{10} - 2C'u) = 0. \tag{17}$$

Now we consider the substitution $u = 1/R + \varepsilon$, where ε is an infinitesimal quantity, so that Eq. 16 gives

$$\frac{d^2\varepsilon}{d\theta^2} - \frac{m}{h^2}\left(\frac{20A'}{R^3} - \frac{110B'}{R^9} - 2C'\right)\varepsilon = 0. \tag{18}$$

For ε to be convergent, it is obvious that the following inequality has to be satisfied $2C'R^9 - 20A'R^6 + 110B' > 0$, where from the definition of C' and the conservation of angular momentum of the system, we find $R < (33B'/5A')^{1/6}$. In addition, the boundness of the atom at $r = R$ or $V_{eff} < 0$ has to be checked. From Eq. 11, this gives the following condition

$$\frac{C'}{R^2} - \frac{A'}{R^5} + \frac{B'}{R^{11}} < 0 \Rightarrow R < \left(\frac{3B'}{A'}\right)^{1/6}. \tag{19}$$

Therefore, R must satisfy the following criteria for the atom orbiting in its stable and bounded circular orbit

$$R < \min\left\{\left(\frac{33B'}{5A'}\right)^{1/6}, \left(\frac{3B'}{A'}\right)^{1/6}\right\} = \left(\frac{3B'}{A'}\right)^{1/6} \approx 3.8\ \text{Å}. \tag{20}$$

Upon taking $R = 3.8\,\text{Å}$, the circular orbiting frequency can be estimated to be $f = 29$ GHz by utilizing Eq. 15. Given the circular orbiting frequency, the angular kinetic energy can be easily calculated as $0.074/r^2$ eV by fixing the angular momentum of the system $h = 5.4 \times 10^{-14}\ \text{kg m}^2\text{s}^{-1}$, and the effective potential energy V_{eff} can then be computed by incorporating the angular kinetic energy. For comparison, we plot the angular kinetic energy, the molecular potential energy and the effective potential energy, as shown in Fig. 2. The effective potential energy of this system is found to resemble classical planetary motion and all possible classifications of the atom's loci can be explained in terms of its total energy. Note that the circular orbiting radius R, estimated in Eq. 20, agrees with the value of R suggested from Fig. 2. For an atom to stay orbiting in its circular orbit, the total energy must be equal to the minimum energy configuration of the effective potential energy V_{eff}, namely

$$E = \frac{B'}{R^{11}} - \frac{A'}{R^5} - \frac{C'}{R^2} \approx -1.14\ \text{meV}. \tag{21}$$

3.2 Numerical locus for atom–carbon nanotube system

In this section, numerical solutions for the loci of Eq. 14 is determined. For a given value of angular momentum of the system h, we examine the conditions for which the atom's orbit is either bounded or unbounded. From Eq. 14, we have

$$\frac{du}{d\theta} = \pm\frac{\sqrt{E - B'u^{11} + A'u^5 - C'u^2}}{\sqrt{C'}}, \tag{22}$$

so that if we discretize a complete revolution into N grid points then a first order numerical scheme, utilizing Euler's method [18], is given by

$$u_{i+1} = u_i \pm \varepsilon \frac{\sqrt{E - B'u_i^{11} + A'u_i^5 - C'u_i^2}}{\sqrt{C'}}, \tag{23}$$

where $i \in [1, N]$, $\varepsilon = 2\pi/N$ and N is the total number of grid points. For Eq. 23 to have real solutions, $E \geq B'u_i^{11} - A'u_i^5 + C'u_i^2$ is required to be satisfied for all i. In particular, when $E = B'u_0^{11} - A'u_0^5 + C'u_0^2$, $u_{i+1} = u_i$ for all i and this corresponds to a circular orbit. The constant C' is taken to be 0.074 and this numerical scheme is carried out for different values of the total energy E.

In this paper, unless otherwise stated, we apply the numerical scheme to 20 revolutions of the orbiting atom, where 100 grid points are utilized. Owing to the feature of the effective potential energy in Fig. 2, one dip and one crest are observed, where the crest's tail goes to infinity. Therefore, we consider $E = -1.14$, -0.6, 0, 0.5 and 1.1 meV, where -1.14 meV is the value of E at the dip of V_{eff}, -0.6 meV is the mid-point between 0 eV and the dip, 0.5 meV is the mid-point between the crest and the zero potential and 1.1 meV is the crest's energy. For a given total energy E, feasible initial positions are determined utilizing the expression $E = (1/2)mv^2 + V_{eff}$, for which the velocity is real if and only if $E \geq V_{eff}$. The numerical outcomes are presented below with physical explanations.

Case 1 ($E = -1.14$ meV): In this case (see Fig. 3), the only possible initial position r_0 is the atom's own circular orbit, which is equal to $R = 3.8$ Å. All other values of r_0 gives rise to $E < V_{eff}$, which is not physically feasible.

Case 2 ($E = -0.6$ meV): In this case, possible initial positions r_0 lie between 3.58 and 4.191 Å, which are determined numerically by solving r from $V_{eff} = -0.6$. An orbit with this total energy is clearly bounded between 3.58 and 4.191 Å, which corresponds to an elliptic orbit (where here we define an elliptic orbit to be an orbit that is bounded by two different radii). Therefore, three initial positions, namely 3.6, 3.8 and 4 Å have been examined (see Fig. 4). From the figure, it is clear that any carbon atom with this total energy departs from its initial positions and then oscillates between the two

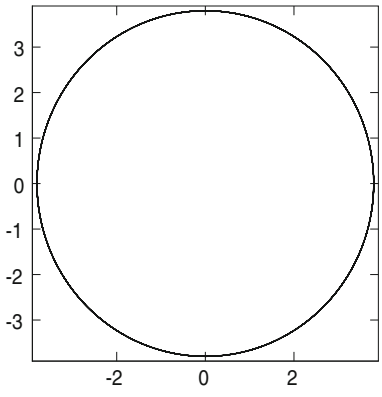

Fig. 3 Locus for $E = -1.14$ meV with initial position 3.8 Å. Atom is orbiting in its stable circular orbit

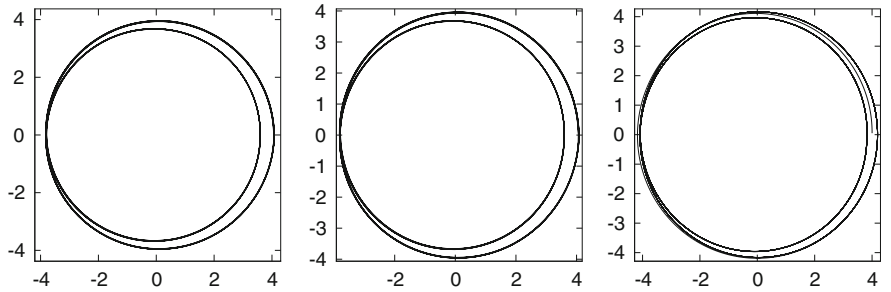

Fig. 4 Loci for $E = -0.6$ meV with initial positions 3.6, 3.8 and 4 Å from left to right respectively. Atom is bounded between 3.58 and 4.191 Å for all these initial positions

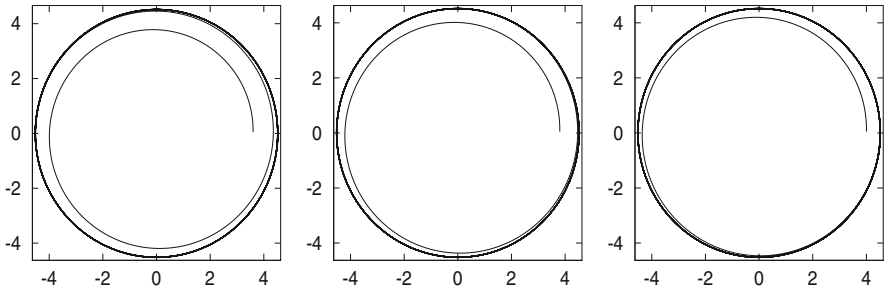

Fig. 5 Loci for $E = 0$ eV with initial positions 3.6, 3.8 and 4 Å from left to right respectively. Atom is swirling away from its bounded loci gradually for all these initial positions

boundaries $r = 3.58$ and $r = 4.191$ Å, which indicates that the molecular potential energy is strong enough to hold the atom in a bounded orbit but weak enough to keep it in a stable circular orbit.

Case 3 ($E = 0$ eV): In this case, r_0 lies between 3.504 and 4.509 Å. Unlike the previous cases, orbiting motion involving this energy level are bounded but unstable, owing to the fact that a point at infinity is also an initial accessible point. This form of locus corresponds to a parabolic orbit (where here we define a parabolic orbit to be an orbit such that an atom orbits to the outer-shell radius and then swirls away to infinity gradually). Similar to the second case, 3 initial positions have been chosen to examine, namely 3.6, 3.8 and 4 Å (see Fig. 5). It is clear that an atom will move away from its initial positions to the outer boundary $r = 4.509$ Å and then gradually swirls away to infinity.

Case 4 ($E = 0.5$ meV): In this case, r_0 lies between 3.46 and 4.86 Å and between 11.765 Å and infinity. In particular, the boundness of an atom's orbit depends heavily on its initial positions r_0. If $3.46\,\text{Å} \leq r_0 \leq 4.86\,\text{Å}$, its locus is elliptic, which is bounded, while if $r_0 \geq 11.765$ Å, its locus is a hyperbolic orbit (where here we define a hyperbolic orbit to be an orbit such that an atom swirls away from the nanotube quickly), which is unbounded. Four initial positions, namely 3.6, 3.8, 4 and 12 Å, have been examined (see Figs. 6 and 7). For $r_0 = 3.6$, 3.8, 4 Å, an atom departs from its initial positions and then oscillates between the two boundaries $r = 3.46$ and $r = 4.86$ Å. However, for $r_0 = 12$ Å, the numerical scheme is unstable, even in

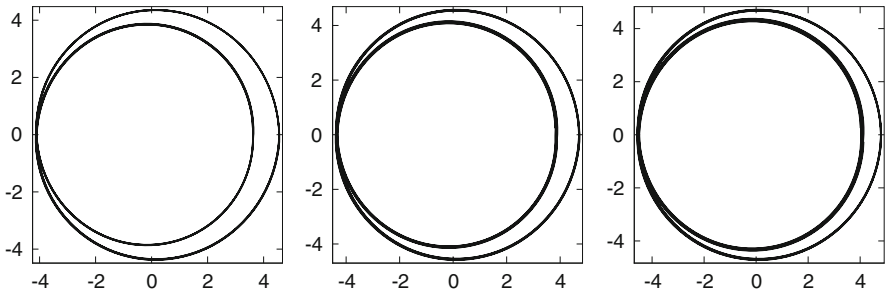

Fig. 6 Loci for $E = 0.5$ meV with initial positions 3.6, 3.8 and 4 Å from left to right respectively. Atom is oscillating between $r = 3.46$ Å and $r = 4.86$ Å for all these initial positions

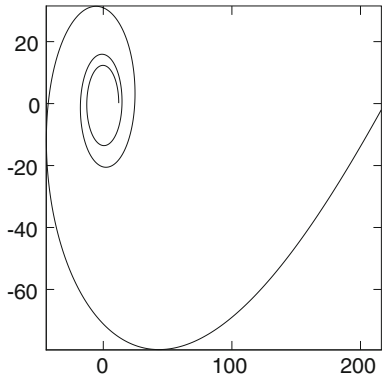

Fig. 7 Locus for $E = 0.5$ meV with initial position 12 Å. Atom escapes from its initial position to infinity very quickly

the third revolution, which indicates that the molecular potential energy is too weak to hold the atom in a bounded orbit and the atom escapes from its initial position to infinity quickly.

Case 5 ($E = 1.1$ meV): In this case, $r_0 \geq 3.42$ Å and the atom's locus is an hyperbola, which is unbounded. Two initial positions, namely 3.8 and 10 Å, have been examined (see Fig. 8). For $r_0 = 3.8$ Å, the numerical scheme becomes unstable after 10 revolutions, while for $r_0 = 10$ Å the numerical scheme becomes unstable even after two revolutions. Therefore, the atom swirls away from its initial position to infinity for all accessible initial positions.

3.3 Perturbation solution for atom–carbon nanotube system

We suppose that an atom is introduced from infinity to a regime, where the attractive forces dominate. This assumption is particularly valid when the 6–12 Lennard–Jones potential is replaced by the hard-sphere repulsive potential given by Hirschfelder et al. [19], namely

$$V(\rho) = \begin{cases} -\frac{D}{\rho^6} & r > \sigma, \\ \infty & r \leq \sigma, \end{cases} \tag{24}$$

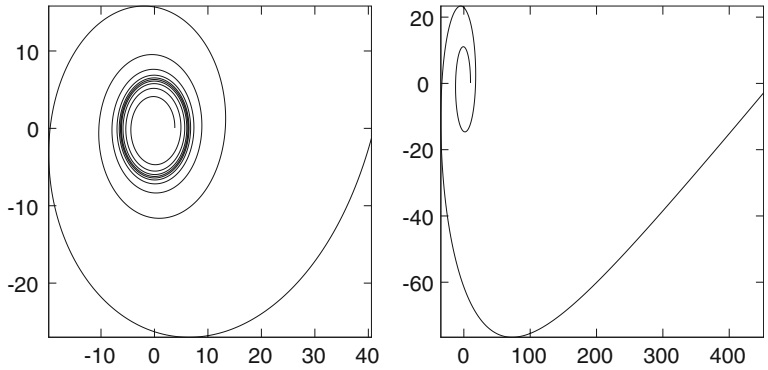

Fig. 8 Loci for $E = 1.1$ meV with initial positions 3.8 and 10 Å from left to right respectively. Atom escapes from its initial position to infinity very quickly for all these initial positions

where D and σ are the modified attractive constant and the collision diameter respectively. At infinity, the total energy is simply equal to the atom's kinetic energy, and this initial energy helps the atom to gain its initial angular momentum orbiting around the carbon nanotube. According to this assumption, the total energy can be represented by $E = E_0 + \varepsilon E_1 + \varepsilon^2 E_2 + \cdots$, where E_0 is approximately zero, and ε is a small positive quantity. Initially, only $E = 0$ is considered, so that Eq. 14 gives

$$d\theta = -\sqrt{C'}\frac{du}{\sqrt{A'u^5 - C'u^2}}. \tag{25}$$

It is interesting to note that the above equation is integrable and from [20], Eq. 25 can be integrated to yield

$$r = \left(\frac{A'}{C'}\right)^{1/3} \cos^{2/3}\left[\frac{3}{2}(\theta - \theta_0)\right], \tag{26}$$

where θ_0 is an initial angle and r results from the substitution $u = 1/r$. Equation 26 suggests that without the initial energy, the atom is captured by the Lennard–Jones potential from infinity. After it encounters a repulsive potential barrier, which is located at the center of the nanotube, it bounces back to an amplitude of $(A'/C')^{1/3}$. Once there, the atom is re-captured by the attractive molecular potential energy and this process repeats periodically and endlessly. The graph of Eq. 26 is plotted in Fig. 9. We note that in Eq. 25, the repulsive energy is ignored. If it is included, r will not reach the center of the carbon nanotube as suggested by Eq. 26 and Fig. 9. Instead, the atom will start to bounce back when it enters the repulsive region of the carbon nanotube.

Now, we construct a small perturbation, i.e. $E = \varepsilon E_1 + O(\varepsilon^2)$, so that from Eq. 14 we find

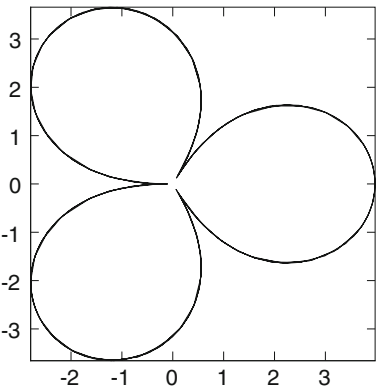

Fig. 9 Orbiting path described by Eq. 26

$$d\theta = -\sqrt{C'}\frac{du}{\sqrt{\varepsilon E_1 + A'u^5 - C'u^2}} \approx -\sqrt{\frac{C'}{A'}}\left\{\frac{du}{u\sqrt{u^3-\xi^3}} - \frac{\varepsilon E_1}{2}\frac{du}{u^3(u^3-\xi^3)^{3/2}}\right\}, \tag{27}$$

where $\xi = (C'/A')^{1/3}$. Next, we transform Eq. 27 by making $d\theta = \theta_f - \theta_i$ and $du = u_f - u_i$, where θ_i, u_i, θ_f and u_f denote the initial angle, the initial radius, the final angle and the final radius, respectively. After some manipulation, we find that the evolution equation for r, is given by

$$r_f = H(u_i, E_1)r_i, \tag{28}$$

where $H(u_i, E_1)$ denotes $\Theta(u_i, E_1)/(\Theta(u_i, E_1)-\delta)$ and the expressions for $\Theta(u_i, E_1)$ and δ are

$$\Theta(u_i, E_1) = \frac{1}{\sqrt{u_i^3-\xi^3}} - \frac{\varepsilon E_1}{2}\frac{1}{u_i^2(u_i^3-\xi^3)^{3/2}} = \sqrt{\frac{A'}{C'}}(\theta_f - \theta_i) > 0. \tag{29}$$

We note that when $\Theta(u_i, E_1) = \delta/2$, $|H(u_i, E_1)| = 1$, the atom always stays on the circular orbit. If $|H(u_i, E_1)| > 1$, then the atom moves away from the carbon nanotube, while if $|H(u_i, E_1)| < 1$, then the atom moves towards the carbon nanotube. It can be easily shown that $|H(u_i, E_1)| > 1$ is satisfied whenever $\Theta(u_i, E_1) > 0$, except for the case of $\Theta(u_i, E_1) = \delta/2$, whereas $|H(u_i, E_1)| < 1$ is satisfied whenever $\Theta(u_i, E_1) < 0$. Given that, we can determine the minimum circular energy E_R by solving $\Theta(u_i, E_c) = \delta/2$ and the cut-off energy E_c by solving $\Theta(u_i, E_c) = 0$, thus

$$E_c = -\frac{2u_i^2}{\varepsilon}(\xi^3 - u_i^3), \qquad E_R = E_c - \frac{\delta u_i^2(u_i^3-\xi^3)^{3/2}}{\varepsilon}. \tag{30}$$

It is interesting to note that $E_R < E_c$. For simplicity, we assume here that E_1, E_c and E_R are all negative real numbers. However, this cut-off energy is not sufficient to

determine the atom's loci. For example, if $E_1 > E_c$, then $|H(u_i, E_1)| > 1$ follows. But, it is naive to think that r will always keep increasing, which corresponds to either a parabolic or a hyperbolic orbit. An increment in r may also increase the value of E_c if and only if $u_i < (2/5)^{1/3}\xi$. Assuming that the value of E_1 is sufficiently small such that E_1 falls below E_c, then $|H(u_i, E_1)| < 1$ occurs and the atom will start to move towards the carbon nanotube, which corresponds to an elliptic orbit. Hence, both the initial position and the initial total energy are paramount to determine the atom's loci. Note that in this section, we investigate only a qualitative description of the atom's loci, where the full prediction of its loci can only be determined by solving Eq. 14.

4 Fullerene–carbon nanotube system

In this section, we determine the loci of a fullerene C_{60} orbiting around a (6,6) carbon nanotube of infinite length. To obtain the interaction potential energy between the two molecules, we perform double integrals of the Lennard–Jones potential over the surface of the fullerene and the carbon nanotube. In addition, the classical spinning of a fullerene, which arises from atomic vibrations, is also incorporated into the model to encapsulate the possible physical phenomenon at the nanoscale. Due to the symmetry of the problem, there is a radial force acting between the center of the fullerene and the carbon nanotube, which provides a centripetal force to the fullerene moving around the carbon nanotube, so that the fullerene eventually orbits around the center of mass of the carbon nanotube in a perpendicular plane. Results from the previous atom–carbon nanotube system can be employed in this system. The illustration of this system is shown in Fig. 10, where a, b and r denote the radius of a $(6, 6)$ carbon nanotube, the radius of the fullerene C_{60} and the distance between the center of the carbon nanotube and the center of the fullerene respectively. The molecular potential energy of this system can be written as

$$V = n_g n_f \int_{\Sigma_g} \int_{\Sigma_f} \left(-\frac{A}{\rho^6} + \frac{B}{\rho^{12}} \right) d\Sigma_f d\Sigma_g, \tag{31}$$

where n_g, n_f and ρ denote the mean surface density of atoms on the carbon nanotube, the mean surface density of atoms on the fullerene, and the distance between an atom on the fullerene and an atom on the carbon nanotube, respectively. In addition, $d\Sigma_f$ and $d\Sigma_g$ denote the surface area segments of the fullerene and the carbon nanotube, respectively. Following Mahanty and Ninham [21] and Ruoff and Hickman [22], the potential energy for an atom interacting with a fullerene of radius b can be deduced as $P(\rho) = -Q_6(\rho) + Q_{12}(\rho)$, where $Q_n(\rho)$ is defined by

$$Q_n = \frac{2C_n n_f \pi b}{\rho(2-n)} \left\{ \frac{1}{(\rho+b)^{n-2}} - \frac{1}{(\rho-b)^{n-2}} \right\}, \tag{32}$$

where the constants C_6 and C_{12} denote A and B, respectively. By performing another surface integral over the surface of the carbon nanotube, the molecular potential energy becomes

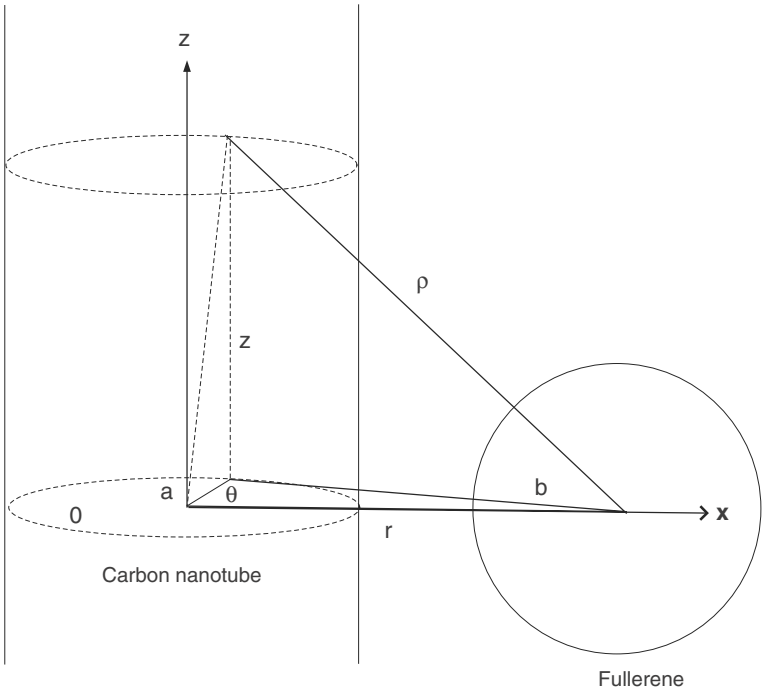

Fig. 10 Fullerene orbiting around a carbon nanotube

$$V(\rho) = n_g a \int_{-\infty}^{+\infty} \int_0^{2\pi} P d\theta dz$$
$$= n_g n_f \pi ab \int_{-\infty}^{+\infty} \int_0^{2\pi} \frac{1}{\rho} \left(\frac{A}{2} \left[\frac{1}{(\rho+b)^4} - \frac{1}{(\rho-b)^4} \right] - \frac{B}{5} \left[\frac{1}{(\rho+b)^{10}} - \frac{1}{(\rho-b)^{10}} \right] \right) d\theta dz, \tag{33}$$

where $\rho = \sqrt{\lambda^2 + z^2}$ and $\lambda = \sqrt{r^2 - 2ar\cos\theta + a^2}$. Upon integrating Eq. 33, we obtain

$$V(r) = 16 n_g n_f \pi ab[-A(bJ_3 + 2b^3 J_4) + \frac{1}{5}(5bJ_6 + 80b^3 J_7 + 336b^5 J_8 + 512b^7 J_9 + 256b^9 J_{10})], \tag{34}$$

where

$$J_n = \frac{(2n-3)!!\pi^2}{(2n-2)!!} \frac{F(n-1/2, 1/2; 1; -4ar/[(r-a)^2 - b^2])}{[(r-a)^2 - b^2]^{n-1/2}},$$

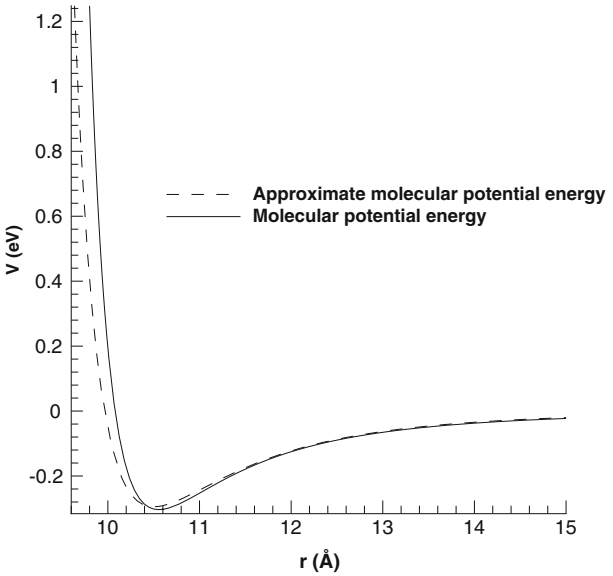

Fig. 11 Molecular potential energy (34) and its approximation (35) for fullerene–carbon nanotube system

and !! represents the double factorial notation such that $(2n-1)!! = (2n-1)(2n-3)\ldots 3\cdot 1$ and $(2n)!! = (2n)(2n-2)\ldots 4\cdot 2$. It is easy to observe from Eq. 34 that the molecular potential energy has a singularity at $r = a + b$ owing to the repulsive potential energy from the Lennard–Jones potential. The molecular potential energy of the system is plotted in Fig. 11.

We note that the behaviour of the potential energy (34) is similar to that of the atom–carbon nanotube system. However, the potential well is two orders of magnitude larger than that of the atom–carbon nanotube system. This indicates that this system would be less sensitive to any thermal fluctuations arising from the environment. It is therefore expected that experimentally, the orbiting behavior of a fullerene can be observed easier than that of a single atom. Assuming that all the thermal energy, which is equal to the potential difference between the zero potential and the dip, is converted into the kinetic energy of the fullerene, the escape velocity is estimated to be 287.31 ms^{-1}, which can be achieved in laboratories by liquid helium cooling [23]. To simplify our analysis, if $a < r$ and only the lowest order of b is considered, then Eq. 34 reduces to a potential form, which is similar to the atom–carbon nanotube system, namely

$$V(r) = -\frac{A''}{[(r-a)^2 - b^2]^{5/2}} + \frac{B''}{[(r-a)^2 - b^2]^{11/2}}, \tag{35}$$

where $A'' = 6n_g n_f \pi^3 ab^2 A = 24 \times 10^2\,\mathrm{eV\,\AA}^4$ and $B'' = 39.375 n_g n_f \pi^3 ab^2 B = 0.26 \times 10^8\,\mathrm{eV\,\AA}^{10}$ are modified attractive and repulsive constants respectively. As shown in Fig. 11, the approximate potential energy (35) is in good agreement with the actual molecular potential energy (34).

Owing to the symmetry of this problem, the results in the atom-carbon nanotube system can be readily extended to this system by utilizing the substitution of $R \rightarrow \sqrt{(R-a)^2 - b^2}$. According to Eq. 20, the threshold circular orbiting radius of this system, which is bounded and stable, is given by

$$\sqrt{(R-a)^2 - b^2} = \left(3B''/A''\right)^{1/6} = 5.6\ \text{Å} \Rightarrow R = 10.7\ \text{Å}. \tag{36}$$

The orbiting frequency of the fullerene can be calculated utilizing Eq. 15, and is equal to $f = 4$ GHz, given that the angular momentum of the system h is equal to 3.44×10^{-12} kg m^2 s^{-1}. In addition, the fullerene's angular kinetic energy can be computed to be equal to $5/r^2$ eV. The angular kinetic energy, molecular potential energy and effective potential energy for a C_{60}–carbon nanotube system are plotted together in Fig. 12 for comparison. Since the angular kinetic energy in this system is small in comparison to the molecular potential energy, the effective potential energy is essentially the same as the molecular potential energy and this gives rise to a different interpretation of the classification of loci in comparison to the atom–carbon nanotube system. In particular;

- the fullerene is in a circular orbit, which is bounded at the potential well of V_{eff},
- when the total energy of the fullerene increases but remains below 0 eV, the fullerene's locus is elliptic, which is bounded,
- when its total energy equals 0 eV, its locus is parabolic, which is unbounded,
- when its total energy becomes strictly positive, its locus is hyperbolic, which is unbounded.

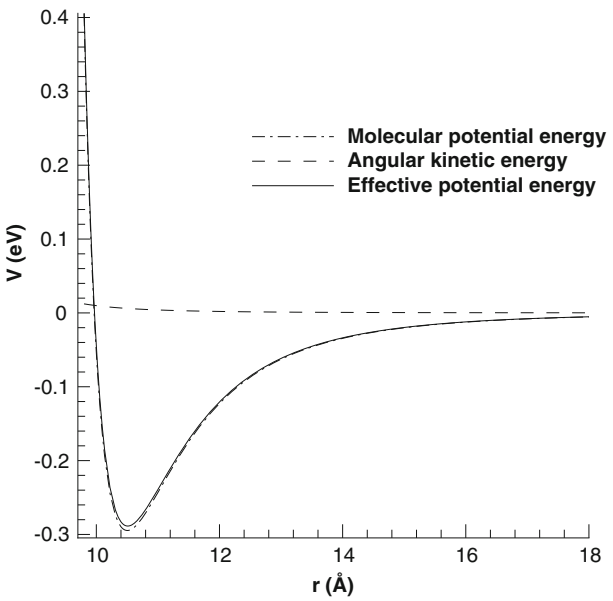

Fig. 12 Fullerene's angular energy, ensemble molecular energy and effective potential energy

Finally, the classical spinning effect of the fullerene may be incorporated into the model. Since the fullerene can spin due to the atomic vibrations at the nanoscale, the spinning kinetic energy may be written as $I\omega^2/2$, where $I = 2m_1b^2/3$ and ω are the moment of the inertia and the spinning frequency of the C_{60} molecule, respectively. The presence of the spinning shifts the effective potential energy upward by the amount of $I\omega^2/2$, however the analysis to determine the fullerene's locus is principally the same as shown in this paper.

5 Fullerene–fullerene system

In this section, we study the orbiting of a fullerene C_{60} around a fullerene C_{1500}. An illustration of this system is given in Fig. 13. The fullerene C_{1500} is chosen due to the fact that the center of mass of this system coincides with the center of the C_{1500} fullerene, which therefore simplifies our calculations. The solution method for this system is very similar to the fullerene–carbon nanotube system. However, due to the spherical symmetry of this system, the molecular potential energy can be obtained in a simpler manner because the axis of the line joining the centers of the two fullerenes can be aligned with the z-axis of the larger fullerene, and the molecular potential energy of the system becomes

$$V(\rho) = n_1 n_2 \pi b \int_{S2} \frac{1}{\rho} \left\{ \frac{A}{2} \left[\frac{1}{(\rho+b)^4} - \frac{1}{(\rho-b)^4} \right] - \frac{B}{5} \left[\frac{1}{(\rho+b)^{10}} - \frac{1}{(\rho-b)^{10}} \right] \right\} d\Omega_2, \tag{37}$$

where n_1 and n_2 denote the mean surface densities of atoms on the C_{60} and the C_{1500} fullerenes, respectively. By exploring the symmetry of this system, the orbital radius r

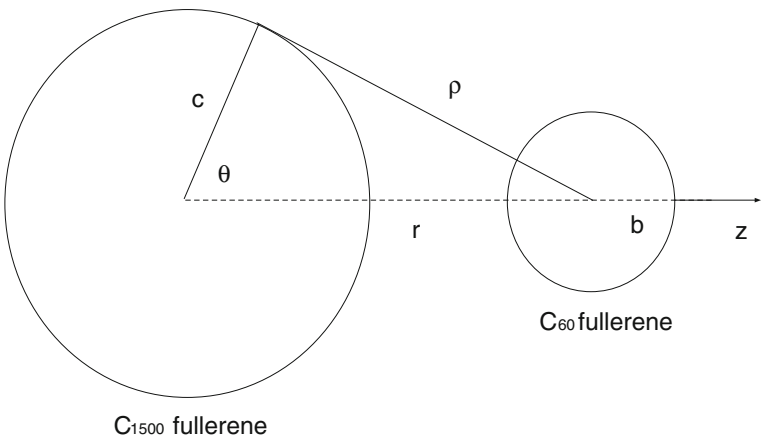

Fig. 13 Geometry of a C_{60} molecule orbiting around a C_{1500} fullerene

can be aligned with the z-axis of the larger fullerene C_{1500}. Hence, from the cosine law we have $\rho = \sqrt{c^2 + r^2 - 2cr\cos\theta}$. By performing the integration over the surface of C_{60} and C_{1500} fullerenes, the molecular potential energy $V(\rho)$ becomes

$$V(\rho) = 2\pi^2 n_1 n_2 c^2 b \int_{\theta=0}^{\pi} \left\{ \frac{A}{2\rho} \left[\frac{1}{(\rho+b)^4} - \frac{1}{(\rho-b)^4} \right] - \frac{B}{5\rho} \left[\frac{1}{(\rho+b)^{10}} - \frac{1}{(\rho-b)^{10}} \right] \right\} \sin\theta d\theta, \tag{38}$$

where c denotes the radius of the C_{1500} fullerene and employing similar calculation as of the fullerene–carbon nanotube system, we find

$$V(r) = 8n_1 n_2 \pi^2 b^2 c^2 \left[-A\left(J_3 + 2b^2 J_4\right) + \frac{B}{5}(5J_6 + 80b^2 J_7 + 336b^4 J_8 + 512b^6 J_9 + 256b^8 J_{10}) \right], \tag{39}$$

where

$$J_n = \frac{1}{2c(n-1)r} \left\{ \frac{1}{[(r-c)^2 - b^2]^{n-1}} - \frac{1}{[(r+c)^2 - b^2]^{n-1}} \right\}.$$

The molecular potential energy is plotted as shown in Fig. 14.

We observe that this energy becomes singular at $r = b + c$, similar to that of the fullerene–carbon nanotube system. Further, the circular orbiting radius in this sys-

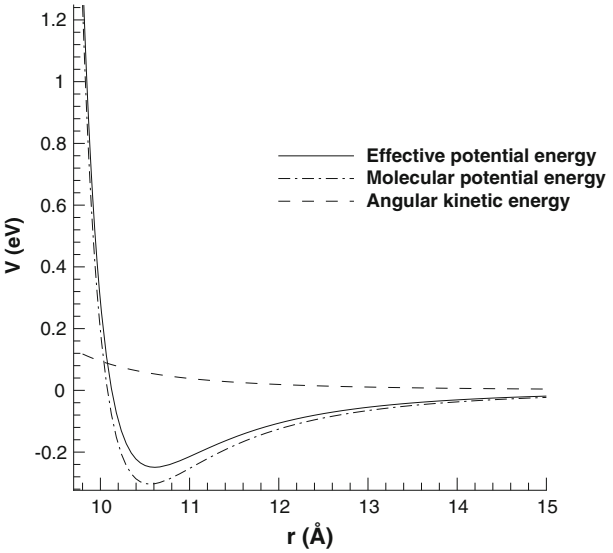

Fig. 14 Molecular potential energy, angular kinetic energy and effective potential energy for C_{60}–C_{1500} system

tem becomes very close to the radius obtained directly by minimizing the molecular potential energy alone. Therefore, according to Fig. 14, the circular orbiting radius can be readily read off as $R = 24\,\text{Å}$ and the orbiting frequency is calculated as

$$f = \frac{1}{2\pi}\sqrt{\frac{V'(R)}{m_1 R}} = 1.6\,\text{GHz}, \tag{40}$$

where m_1 is the total mass of the C_{60} molecule. The angular kinetic energy, which is given by $24.5/r^2\,\text{eV}$, and the effective potential energy are plotted together with the molecular potential energy in Fig. 14. Similar to the fullerene–carbon nanotube system, the classical spinning effect can also be incorporated in this system and the classification of loci can be similarly examined. This orbiting effect may be detected experimentally since the fullerene's escape velocity is calculated to be $365.76\,\text{ms}^{-1}$.

6 Conclusion

In this paper, three two-body nanoscale problems are examined, namely an atom–carbon nanotube system, a fullerene–carbon nanotube system and a fullerene–fullerene system. The effective potential energy of these proposed systems are found to be similar to the classical planetary potential energy, which suggests that these nano-systems possess orbiting phenomenon. The circular orbiting radii of all the proposed nano-systems are estimated by seeking the minimum energy configuration of their effective potential energies and a stability and a boundness analysis is performed close to a perfect circular orbit to determine the stability of the circular orbits. Since the loci for these nano-systems cannot be determined in terms of well-known analytical functions, a numerical method has been employed to obtain the various loci of the orbiting paths. In addition, a perturbation method has been utilized in order to gain some insight into possible analytical formulations of the loci. Most importantly, the circular orbiting frequencies of all three proposed nano-systems reach the gigahertz range, which suggests that these nano-systems can be utilized as future nanoscale devices, such as nano-motors and nano-signal generators. We comment that this paper does not incorporate the effect of thermal fluctuations arising from the environment, which could certainly disrupt the orbiting behavior for such nanoscale objects.

Acknowledgements We gratefully acknowledge the support from the Discovery Project Scheme of the Australian Research Council.

References

1. S. Iijima, Helical microtubules of graphitic carbon. Nature **354**, 56 (1991)
2. J. Cumings, A. Zettl, Low-friction nanoscale linear bearing realized from multiwall carbon nanotubes. Science **289**, 602 (2000)
3. M.F. Yu, B.I. Yakobson, R.S. Ruoff, Controlled sliding and pullout of nested shells in individual multiwalled carbon nanotubes. J. Phys. Chem. B **104**, 8764 (2000)
4. Q. Zheng, Q. Jiang, Multiwalled carbon nanotubes as gigahertz oscillators. Phys. Rev. Lett. **88**, 045503 (2002)

5. S.B. Legoas, V.R. Coluci, S.F. Braga, P.Z. Coura, S.O. Dantas, D.S. Galvao, Molecular-dynamics simulations of carbon nanotubes as gigahertz oscillators. Phys. Rev. Lett. **90**, 055504 (2003)
6. J.L. Rivera, C. McCabe, P.T. Cumming, Oscillatory behavior of double nanotubes under extension: a simple nanoscale damped spring. Nano Lett. **3**, 1001 (2003)
7. J.L. Rivera, C. McCabe, P.T. Cumming, The oscillatory damped behaviour of incommensurate double-walled carbon nanotubes. Nanotechnology **16**, 186 (2005)
8. D. Baowan, J.M. Hill, Accurate expressions for the force distribution for double-walled carbon nanotubes. Z. Angew. Math. Phys. **58**, 857 (2007)
9. P. Liu, Y.W. Zhang, C. Lu, Oscillatory behavior of C_{60}-nanotube oscillators: a molecular-dynamics study. J. Appl. Phys. **97**, 094313 (2005)
10. D. Qian, W.K. Liu, R.S. Ruoff, Mechanics of C_{60} in nanotubes. J. Phys. Chem. B. **105**, 10753 (2001)
11. B.J. Cox, N. Thamwattana, J.M. Hill, Mechanics of atoms and fullerenes in single-walled carbon nanotubes. I. Acceptance and suction energies. Proc. R. Soc. Lond. A **463**, 461 (2007)
12. B.J. Cox, N. Thamwattana, J.M. Hill, Mechanics of atoms and fullerenes in single-walled carbon nanotubes. II. Oscillatory behaviour. Proc. R. Soc. Lond. A **463**, 477 (2007)
13. B.J. Cox, N. Thamwattana, J.M. Hill, Mechanics of nanotubes oscillating in carbon nanotube bundles. Proc. R. Soc. Lond. A **646**, 691 (2008)
14. B.J. Cox, N. Thamwattana, J.M. Hill, Mechanics of fullerenes oscillating in carbon nanotube bundles. J. Phys. A: Math. Theor. **40**, 13197 (2007)
15. T.A. Hilder, J.M. Hill, Orbiting nanosectors inside carbon nanotori. Micro Nano Lett. **2**, 50 (2007)
16. T.A. Hilder, J.M. Hill, Orbiting atoms and C_{60} fullerenes inside carbon nanotori. J. Appl. Phys. **101**, 064319 (2007)
17. H. Goldstein, C. Poole, J. Safko, *Classical Mechanics* (Addison Wesley, RiverPearson, 2002)
18. R.L. Burden, J.D. Faires, *Numerical Analysis* (Thomson, South Bank, 2005), p. 257
19. J.O. Hirschfelder, C. Curtiss, R.B. Bird, *Molecular Theory of Gases and Liquids* (Wiley, New York, 1954)
20. M.R. Spiegel, J. Liu, *Mathematical Handbook of Formulas and Tables* (McGraw-Hill International Editions, Singapore, 1999)
21. J. Mahanty, B.W. Ninham, *Dispersion forces* (Academic Press, New York, 1976)
22. R.S. Ruoff, A.P. Hickman, Van der Waals binding to fullerenes to a graphite plane. J. Phys. Chem. **97**, 2494 (1993)
23. A.V. Schneidemesser, G. Thummes, C. Heiden, Generation of liquid helium temperatures using a lead regenerator in a GM precooled pulse tube stage. Cryogenics **40**, 67 (2000)